Ocean Engineering 203 (2020) 107198

Contents lists available at ScienceDirect

Ocean Engineering

journal homepage: www.elsevier.com/locate/oceaneng

A low-cost GNSS buoy platform for measuring coastal sea levels

Philip J. Knight [a,*], Cai O. Bird [b], Alex Sinclair [b], Andrew J. Plater [a]

[a] Department of Geography and Planning, School of Environmental Sciences, Roxby Building, University of Liverpool, United Kingdom
[b] Marlan Maritime Technologies Ltd, 323 Mariners House, Queens Dock Business Centre, Norfolk Street, Liverpool, United Kingdom

ARTICLE INFO

Keywords:
GNSS
Buoy
Sea level
Tide
Seiche

ABSTRACT

A low-cost Global Navigation Satellite System (GNSS) buoy platform was developed for measuring coastal sea levels to provide information where logistical, physical and/or financial constraints prevent the application of established tide gauges and satellite altimetry, and where spatially and temporally discrete tidal data are required to support surveys for monitoring coastal morphodynamics. The buoy was constructed from scaffold tubing and four floats, with a central platform for the GNSS receiver and antenna. The overall cost was around £300 (buoy parts £100, GPS/logger £200). The single frequency GNSS receiver was set up to record GPS/GLONASS satellite data at 5Hz. Post-processing was carried out with RTKLIB software to derive solutions for sea level. GNSS buoy performance was evaluated against a reference tide gauge using a Van de Casteele test. The RMSE of 1.4 cm, computed from the differences between the GNSS-buoy and reference tide gauge, demonstrates that this low-cost GNSS buoy tide gauge compares well with previous, more expensive GNSS buoys and is suitable for obtaining local-scale coastal sea level data. In addition to providing coastal data at cm accuracy, the results also indicate the presence of high frequency oscillations in the sea level data caused by coastal geometry and wave-induced disturbance.

1. Introduction

Obtaining local sea level data is a critical challenge for assessing risks to increasing coastal populations, infrastructure, economies and ecosystems, particularly with respect to characterizing environmental response to projected climate change, storms and sea level rise (cf. Nicholls et al., 2007). This is especially important for low-latitude, small island developing states (SIDS) where the economy is highly reliant upon sustainable development in the low-lying coastal hinterland and adjacent waters, both of which are vulnerable to tropical storms and hurricanes (cf. Turvey, 2007). More widely, data on local sea level can be used to quantify biases and errors due to land contamination of satellite altimetry coastal sea level data, to assure safe port operations and navigation, to underpin accurate flood hazard assessment and forecasting, and to facilitate the assessment of coastal response to hydrodynamic forcing (Marcos et al., 2019) - and thus has an essential role to play in climate change adaptation. Amongst the technologies available for coastal sea level measurement, GNSS buoy platforms provide an effective means for quantifying local sea level, independent of land level, at cm accuracy (Andre et al., 2013). Here, we describe the development and testing of a low-cost GNSS buoy for deployment where local sea level data are required or where tide gauges or satellite altimetry cannot be utilised.

Local sea level data are important for repeat surveys of coastal bathymetry and morphodynamics, which provide essential data on the character of coastal/nearshore change – including quantification of long-term accretion/recession rates, monitoring impacts of engineering interventions and dredging operations, and assessment of response to inter-annual and seasonal variability, and storm forcing (Harley et al., 2011). Furthermore, repeat surveys at smaller spatial and shorter temporal scales provide a foundation for assessing the local implications of global sea level rise projections (Nicholls et al., 2007). Progressing beyond the established application of periodic LiDAR, differential GPS and Unmanned Aerial Vehicle (UAV) surveys, marine X-Band radar allows continuous monitoring of coastal morphology and morphological change over timescales from days to years (Bell, 2008; Bird et al., 2017). Here, the morphology of beaches and tidal flats can be characterised in terms of their instantaneous and long-term behaviours by applying a water-line method (Bell et al., 2016) whereby the advancing and retreating shoreline during the tidal cycle can be assigned an altitude on the basis of the corresponding tidal level. The accuracy of intertidal morphology determined via the water-line method can be significantly

* Corresponding author. School of Environmental Sciences, University of Liverpool, Liverpool, UK.
E-mail address: Philip.Knight@liverpool.ac.uk (P.J. Knight).

https://doi.org/10.1016/j.oceaneng.2020.107198
Received 27 August 2019; Received in revised form 22 January 2020; Accepted 29 February 2020
Available online 10 March 2020

improved when combined with tidal data obtained within the radar survey operating (spatial and temporal) window (Bell et al., 2016). For example, applying the radar water-line method with tidal measurements taken from within the survey domain would reduce any spatial or temporal tidal phase issues that might be present between the survey location and the location of the nearest tide gauge. Furthermore, these portable radar systems may be deployed at coastal locations where local sea level data are not readily available or traditional methods of measuring sea levels cannot easily be applied, e.g., no fixed structures such as piers to attach tide gauges. Thus, GNSS buoy deployment for local sea level at cm accuracy provides an important complement to these new survey technologies.

Global Navigation Satellite System (GNSS) is the standard generic term for satellite navigation systems that provide autonomous geo-spatial positioning with global coverage. This term includes, for example, the US Global Positioning System (GPS), the Russian Global Navigation Satellite System (GLONASS), the European Union Galileo system, the Chinese BeiDou system and other regional systems. GNSS buoys for sea level measurement were originally developed for the verification of data from earth-orbiting satellite altimeters (Hein et al., 1990; Rocken et al., 1990). Essentially, a sea level time-series can be obtained from a GPS antenna mounted on a buoy if the height of the antenna phase centre above sea level is known (Kelecy et al., 1994). GNSS systems use the properties of L-band microwave frequencies, i.e. L1 (1575.42 MHz) and L2 (1227.60 MHz) (Kaplan and Hegarty, 2017) to determine geodetic position from appropriate scaling and combination of the L1 and L2 measurements.

In the past decade, considerable progress has been made on the analysis of reflected GNSS data for sea level monitoring (GNSS-R, e.g. Roussel et al., 2015) but GNSS geodetic receivers are readily deployed on buoy platforms to measure sea surface heights (Watson et al., 2008). For example, Apel et al. (2012) and Frappart et al. (2017) demonstrated how the technology can be applied to buoys in estuarine and river systems, while Lin et al. (2017) showed that by using real time kinematic (RTK) positioning technology, accurate measurements of tidal levels from an offshore buoy could be obtained with a root mean square error (RMSE) of less than 10 cm. Another use of kinematic GNSS at sea is for seafloor geodesy were GNSS buoys have been used in combination with seafloor pressure gauges for vertical deformation monitoring (Ballu et al., 2009). Furthermore, Morales-Maqueda et al. (2016) installed a geodetic GPS on a Wave Glider and used kinematic precise point positioning (PPP) to produce ~5 cm precision water surface heights for a Scottish loch. Later, Penna et al. (2018) used the same Wave Glider configuration with a North Sea deployment and obtained centimetric precision instantaneous sea surface heights, as well as ellipsoidal height estimates and significant wave heights. In another GNSS application, André et al. (2013) compared three geodetic GPS equipped buoys (two recording at 5 Hz and one at 1 Hz) with established radar tide gauge data. They post-processed the GPS data in 'kinematic mode' with respect to a land-based reference station; post-processed kinematic (PPK) mode is an alternative technique to RTK and differs in that the solution algorithms and timing corrections are applied later. The reference station was located around 500 m away from a relatively sheltered coastal location where the buoys were deployed. They concluded that a RMSE range of 1–2.2 cm between the GPS buoys and a radar tide gauge, again evidenced that GPS buoys are suitable for determining coastal sea level. However, Stal et al. (2016) using a similar approach reported an accuracy of 4 cm in a more exposed location and further out to sea. They used a NavCom geodetic GNSS receiver recording at 1 Hz which was fitted to an AXYS Technologies Hydrolevel buoy, with the closest GNSS reference station within 20 km of the deployment. They reported that the data sets suffered noise related to wave heights, and that a significant amount of other noise was present in the positioning solution (see Stal et al. (2016) for further elaboration).

In the examples above, the buoys were fitted with geodetic GNSS receivers and antennas, capable of picking up both the L1 and L2 satellite signals, and recording carrier phase information. These types of receiver can cost between £2000 and £10,000 (GBP), and typically require expensive antennae (~£3000). The advantage of using a L1/L2 receiver is that one of the largest errors (caused by the travel time delays on the satellite signals due to the ionosphere) can be almost eliminated (Kaplan and Hegarty, 2017). Another advantage is that having two simultaneous satellite signals can help in the processing when cycle slips occur in the data (Kaplan and Hegarty, 2017). Furthermore, both the L1/L2 signals are necessary for accurate sea level measurements if using PPP methods, for example when processing data from remote ocean deployments, well away from suitable land-based GNSS reference stations. This paper assesses the performance of an inexpensive GNSS buoy for measuring of sea levels: consisting of a buoy made from readily available parts and a low-priced GNSS receiver and logger, especially as these buoys are intended for deployment in the coastal zone with a potentially high attrition rate. Successful development of this buoy will also have the potential for wider deployment in low and middle income countries where the financial resources for gathering data on coastal hydrodynamics may be limited. First, we compare the derived sea levels with a reference tide gauge, and then investigate the noise in the RTK solutions as reported by Stal et al. (2016). Here, we apply the PPK technique to data from a low cost U-blox M8T GNSS receiver (U-blox, 2019a) with a Tallysman (TW2741) patch antenna. Although limited to the measurement of the L1 signal, it can record the necessary carrier phase information and is capable of centimetre-level accuracies (U-blox, 2016). As well as the lower cost, single L1 receivers also consume less power, which is an advantage for battery/solar-power based applications. Also, their use in the nearshore zone is complemented by land-based GNSS reference stations with geodetic receivers as part of the overall positioning solution.

2. Materials and methods

2.1. Buoy design

The buoy (Fig. 1a) was designed to be easy to construct with 'off the shelf' components (buoy parts total cost ~ £100). The buoy consists of four yellow Polyform Purse Seine floats (BPB Series 4600), four sections of 33 mm diameter aluminium scaffold tubing (three 0.5 m sections and one 1.0 m section), one four-way scaffold connector, two other scaffold tube fittings (one with an eyelet for the mid-section, and one for connecting the mooring line using shackles). The aluminium tubes connect with stainless steel bolts using standard grub-screw holes in the four-way connector, and other fittings as a guide for the drill bit. A black plastic base bolts on to the top of the four-way connector, on which attaches the GNSS package. Each Purse Seine float has a buoyancy capable of supporting a weight of 4.6 kg. The buoy was tested in a local marine lake with different weights to assess the floating profile and its stability in the water. The GNSS receiver electronics and battery (Fig. 1b) were contained in an IP67/68 waterproof enclosure: BOPLA Bocube (270 × 125 × 60 mm). The waterproofing was enhanced using silicon grease on the rubber seals, waterproof tape and flexible sealant for the antenna cable entry.

2.2. GNSS receiver

The U-blox M8T GNSS receiver was chosen as it is a cost-effective, low power unit (~32 mA @ 3 V; just receiver) and has been shown to be capable of centimetre-level accuracies (Ublox, 2016) for land-based RTK applications, including built-up areas where satellite signal losses can occur. It is a single-frequency receiver (capable of receiving the L1 satellite signals) that can record concurrent GPS, GLONASS, BeiDou and Galileo satellite data up to 5 Hz, and up to 10 Hz for single GNSS systems such as GPS. In addition, it records the raw satellite data, including the carrier phase output which is required for the centimetre accuracy. An advantage of the buoy being deployed in a marine environment is that

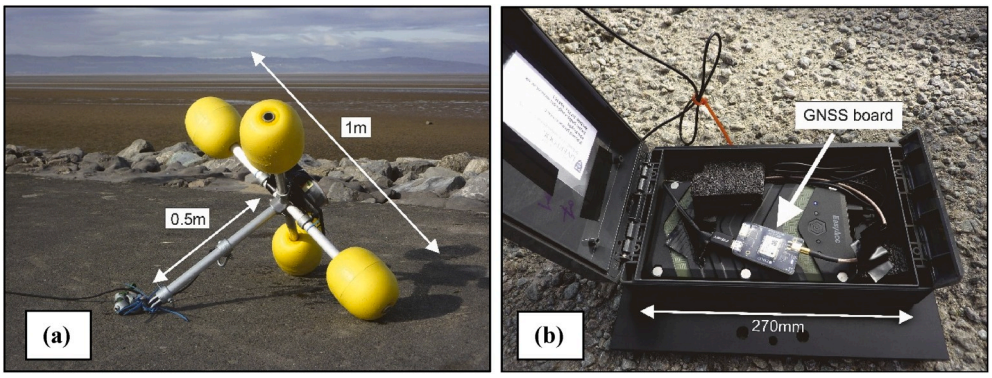

Fig. 1. (a) Buoy design using standard aluminium scaffold tubing and Polyform Purse Seine floats, (b) GNSS package: Emlid Reach Linux board with embedded UBlox M8T GNSS receiver and battery pack.

visibility of the whole sky will be available; while on many land-based applications, such as car tracking, buildings can obscure and scatter the satellite signals. A disadvantage of marine-based deployments is that the buoy will be bounced around with the waves which would induce the losing of low-lying satellite tracking, resulting in inaccurate final horizontal and vertical positioning solutions, as shown by Stal et al. (2016).

The U-blox M8T receiver was first tested using a U-blox evaluation kit (EVK-M8T) with a GNSS logger, though for field-testing, an early Emlid Reach (Emlid Reach, 2019; now updated to the Reach M+, with 8 Gb of memory) was used as it had a M8T receiver already embedded onto a small form Linux board (an Intel Edison), WiFi for data transfer, internal storage (2 Gb) and a software user interface that allowed for quick alteration of the receiver settings. The Emlid Reach (costing ~ £200) includes a small Tallysman multi GNSS patch antenna (TW4721), and is mainly aimed at the growing UAV (drone) market. It is a self-contained experimental package (Fig. 1b) and draws a current of 200–300 mA depending on the set-up and antenna used. The antenna was secured to the top of the enclosure on a 7-cm square steel ground plane. The ground plane is essential to reduce multi-path reflections and increase the antenna gain (U-blox, 2019b); its optimum dimensions (often supplied with antenna manufacturer's specifications) are determined by the antenna size.

An EasyAcc 20,000 mAh battery pack was used with the Emlid

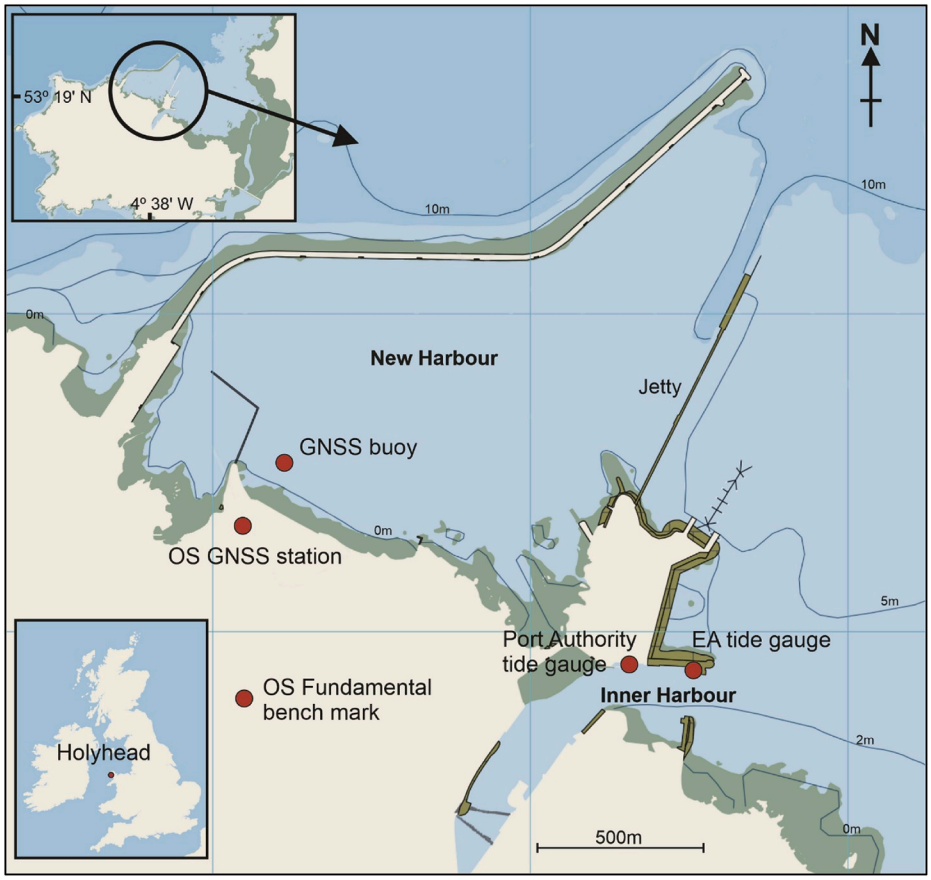

Fig. 2. Location of Holyhead Harbour (North Wales, UK); GNSS buoy, Ordnance Survey GNSS station, Holyhead Port Authority tide gauge, Environment Agency tide gauge and OS fundamental benchmark. The Jetty is open underneath and allows water to pass between the two harbours, although at low tide it is relatively shallow 1–2 m CD. Base map source: EDINA Marine Digimap Service (http://edina.ac.uk/digimap).

Reach, which provided enough power to cover the experimental period; the expected endurance based upon the power requirements would be up to 4 days. Although not part of this initial experiment further successful trials have been carried out using larger capacity batteries as well as Voltaic Systems solar power panels to allow for extended periods of deployment.

2.3. Buoy testing at Holyhead

Holyhead Harbour (Fig. 2) was chosen as the site for the testing as it has a long-established tide gauge (part of the UK National Tide Gauge Network) and an additional Holyhead Port Authority tide gauge for direct comparisons. There is also a UK Ordnance Survey (OS) geodetic GNSS site (WGS: 53° 19′ 03.8″N, 04° 38′ 31.4″W, British National Grid: SH 24104 83343) located at the life boat station close to the New Harbour; a source of research-quality GNSS data which can be applied to the PPK solution, and a fundamental benchmark (WGS: 53° 18′ 47.2″N, 04° 38′ 30.0″W, British National Grid: SH 24111 82829). The datum used throughout is local chart datum (CD) which at Holyhead is 3.05 m below Ordnance Datum Newlyn (ODN). At Holyhead the largest tidal range is 6.26 m (National Oceanography POLTIPS-3, 2019). During the test (11–13 September 2018) the highest predicted tide was 6.16 m while the lowest was 0.21 m, and the largest range was 5.86 m. The highest predicted tide of the month was 6.17 m on 10 September at 22:45; the tides were close to the peak springs, decreasing towards neaps.

The test took place in the New Harbour (Fig. 2) where the buoy was attached to a mooring buoy (Fig. 3) and allowed to float freely (deployed position: WGS: 53° 19′ 08.4″N, 04° 38′ 24.0″W). Charts indicated the mooring location was in about 4 m water depth below chart datum. The U-blox M8T receiver embedded on the Emlid Reach using a Tallysman patch antenna was set up to record GNSS data at 5 Hz; GPS and GLONASS raw satellite data were recorded, including the carrier phase information in the U-blox binary format (ubx). Data were recorded from 10:00 on 11 September until 09:51 on 13 September, with a gap of 42 min (09:35–10:17) on 12 September during a data download test and battery check.

2.4. GNSS data processing

To obtain accurate positions using a moving single-frequency receiver (U-blox M8T), data from another GNSS at a known fixed location are needed (ideally recording both L1 and L2 frequencies), for both RTK and PPK solutions. The open source software RTKLIB (2018) was used for processing the GNSS data. The advantage of PPK over RTK is that the solution can be applied both forwards and backwards in time, and additional corrections for the satellite clocks and orbits can be included as they become available after a few weeks (see below for further details), thus improving the overall positional solution.

Here, the U-blox M8T is the moving rover (the buoy moving in vertical and horizontal directions at the mooring) and the reference OS GNSS is the base station. Optimal solutions for the PPK are obtained as the distances between the rover and base station reduce to within 20 km of each other, thus these have been kept as short as possible for the experiment.

At Holyhead, the distance between the buoy and the reference OS GNSS station was about 200 m (Fig. 2). The OS GNSS station comprises a Trimble Alloy GNSS receiver (capable of receiving the L1 and L2 satellite signals) combined with a Leica AR25 GNSS antenna and data were downloaded from the OS online download facility (Ordnance Survey, 2019). These data are initially available at 30-s intervals and used for initial PPK processing, however, once the 1 Hz data are available (delay of 45 days) these were used in the final positioning solution. The archived 1 Hz GNSS data were obtained from the British Isles continuous GNSS facility BIGF (2018).

The processing uses RTKLIB on data spans of up to six hours (to be within software memory limits); the parameter settings for the software are listed in Table 1. They are mostly the default settings for RTKLIB with recommendations from other groups (for example, Emlid Reach, 2019). They are similar to the optimised settings of Stal et al. (2016) except that 'Sensor dynamics' was switched to ON and GLONASS satellites were used, both of which improve the derived solution. These

Fig. 3. GNSS buoy attached to mooring buoy in Holyhead New Harbour.

Table 1
Parameter settings for the post-processing using RTKLIB.

Parameter	Value
Solution	Kinematic
Frequency	L1
Sensor dynamics	On
Earth tides	Off
Ionosphere	Broadcast
Troposphere	Saastamoinen
Ephemerides	Precise
Satellite system	GPS + GLONASS
Ambiguities GPS	Fix & Hold/Continuous
Ambiguities GLONASS	Off

parameters were used to obtain the best solution for each data period based on the returned RTKLIB solution quality indicators (see RTKLIB manual: RTKLIB, 2018).

To improve the overall solution, satellite ephemerides for precise orbit corrections and satellite and station clock error corrections were applied. These were obtained from the Crustal Dynamics Data Information System (CDDIS, 2018; Noll, 2010). The corrections are delivered with increasing accuracy in the form of 'ultra', 'rapid' and 'final' correction files; available between 3 and 9 h, 17–41 h and 11–17 days, respectively. The results in this paper use the final products.

The GNSS measurements are referred to an 'antenna phase centre': a non-constant value that depends on the direction of the satellite signal i.e., corrections need to be applied during the processing. Within the RTKLIB software package, which outputs the positional data (i.e., including the sea level), there is an option to apply these corrections by including models of the 'antenna phase centre'. These models are available for many of the geodetic antenna types, including the Leica AR25 (base antenna), although not for small low-cost patch antennas such as the TW4721 (rover antenna). Thus, during the processing, the corrections were applied for the Leica AR25 antenna, but not for the TW4721 antenna. Tallysman (2019) provides some antenna performance documentation for the TW4721 which suggests that the 'antenna phase centre' variations fall in a range of 1 cm.

2.5. Local tidal data

Tidal data for comparison with the GNSS buoy results were from the Environment Agency (EA) tide gauge (WGS: 53° 18′ 50.2″N, 04° 37′ 13.6″W, British National Grid: SH 25529 82870) downloaded from British Oceanographic Data Centre (BODC) website www.bodc.ac.uk, and the Holyhead Port Authority's tide gauge (verbal and email communication with the harbour master; WGS: 53° 18′ 50.5″N, 04° 37′ 29.5″W, British National Grid: SH 25233 82889), both in the Holyhead Inner Harbour (Fig. 2). The EA tidal data were recorded as 15-min averages, while the Port Authority tidal data were recorded as one-minute averages. The EA gauge is part of the UK National Tide Gauge Network (UK Coastal Monitoring and Forecasting, 2015) and is the reference tide gauge for this experiment (as BODC monitor the data quality). It consists of a full tide bubbler tide gauge system (Woodworth and Smith, 2003).

3. Results

3.1. GNSS-derived tidal heights and local tide gauge data

Selected comparisons from the data are displayed in Fig. 4 a–e: derived tidal heights to chart datum from the GNSS buoy (5 Hz), Environment Agency tide gauge (15-min averages) and filtered GNSS data (boxcar 15-min moving averages). GNSS data quality is good, with an exception that occurred on 11 September 2018 (23:02–23:10), as illustrated in Fig. 4e. The discontinuity was present when the GNSS receiver recorded fewer quality satellite fixes, hence more uncertainty in the derived position. As the harbour is used 24 h a day and seven days a week, any port traffic nearby could potentially cause 'shadowing' as boats may block some of the satellite signals.

The Fig. 4a and b also show higher frequency signals in the 5 Hz GNSS-derived sea levels (which will be explored in detail in following sections), oscillations of around 10–30 min (which can be attributed to harbour oscillations) and higher frequency oscillations of less than one minute (for example, see Fig. 4a around high water). Fig. 4c and d shows that while the higher frequency oscillations are present in the 5 Hz data, the harbour oscillations are not obvious and seem to have disappeared.

3.2. The Van de Casteele Test

The performance of a tide gauge can be assessed using the Van de Casteele Test. Miguez et al. (2008, 2012) tested a variety of tide gauges and demonstrated the ability to highlight different types of tide gauge error, while André et al. (2013) used it to compare data from three different GNSS buoys for measuring sea level against a nearby radar tide gauge. The method compares a reference tide gauge data set (data known to be an accurate measurement of sea level) to contemporaneous data from the tide gauge being tested (H'): the reference sea level data (H) are plotted on the ordinate against the tide gauge difference (ΔH) on the abscissa (x-axis), where $\Delta H = H - H'$. The resulting diagram would produce a straight vertical line centred on $x = 0$ for a perfect match between the two tide gauges.

3.2.1. Assessing the GNSS buoy tide gauge accuracy

Before comparing the GNSS data with the EA tide gauge data, a 900-s boxcar moving average was applied to the GNSS data, and then values corresponding to the timings of the EA gauge data were resampled at fifteen-minute intervals. The resulting Van de Casteele diagram in Fig. 5a indicates good agreement between the EA tide gauge and the GNSS buoy tide gauge. The near vertical alignment in the chart of the differences between low water and high water, although not perfectively straight, implies that there are no timing offsets (which would result in a more ellipsoidal pattern) and no obvious systematic errors (e.g., scale error; which would have introduced a large gradient from low water to high water), however there is a small overall negative offset from zero. This bias shown in Fig. 5a may be partly due to the spatial difference between the two tide gauges, and/or due to errors in the measurement of the antenna elevation above the water surface. The mean difference between the GNSS data and the EA tide gauge data was −0.011 m, the standard deviation was 0.009 m and the RMSE was 0.014 m. Some of the larger residuals are due to the presence of the harbour oscillations which are noticeable in the 900-s boxcar averaged GNSS data (Fig. 4a), that are not represented in the 15-min EA tide gauge record. These differences may be the result of wave damping that has been introduced within the design of the EA tide gauge bubbler system.

Fig. 6 plots the tidal differences against time (left axis) alongside the EA tide gauge observations (right axis). The time series of differences between tide gauges (ΔH) produces a tide-shaped sinusoid, which is mildly correlated with the tidal cycle; this translates into the small slope (from high tide to low tide) that is evident within the Van de Casteele diagram (Fig. 5a), thus indicating that the GNSS buoy tide gauge is performing well (cf. Miguez et al., 2008).

3.3. Harbour oscillations

To examine the above-mentioned oscillations (with periods of between 10 and 30 min) seen in the 5 Hz data (Fig. 4a), data from the Port Authority tide gauge (recording one-minute averages) were compared to the GNSS-derived sea level data. After applying the Van de Casteele Test (described above) to the Port Authority tidal data using the EA tidal data as the reference, the test results highlight three issues with the Port Authority tide gauge: a general datum offset, a gradient (away from vertical) in the Van de Casteele Test diagram (Fig. 5b) from high water to low water, and large differences at low water. The mean difference was

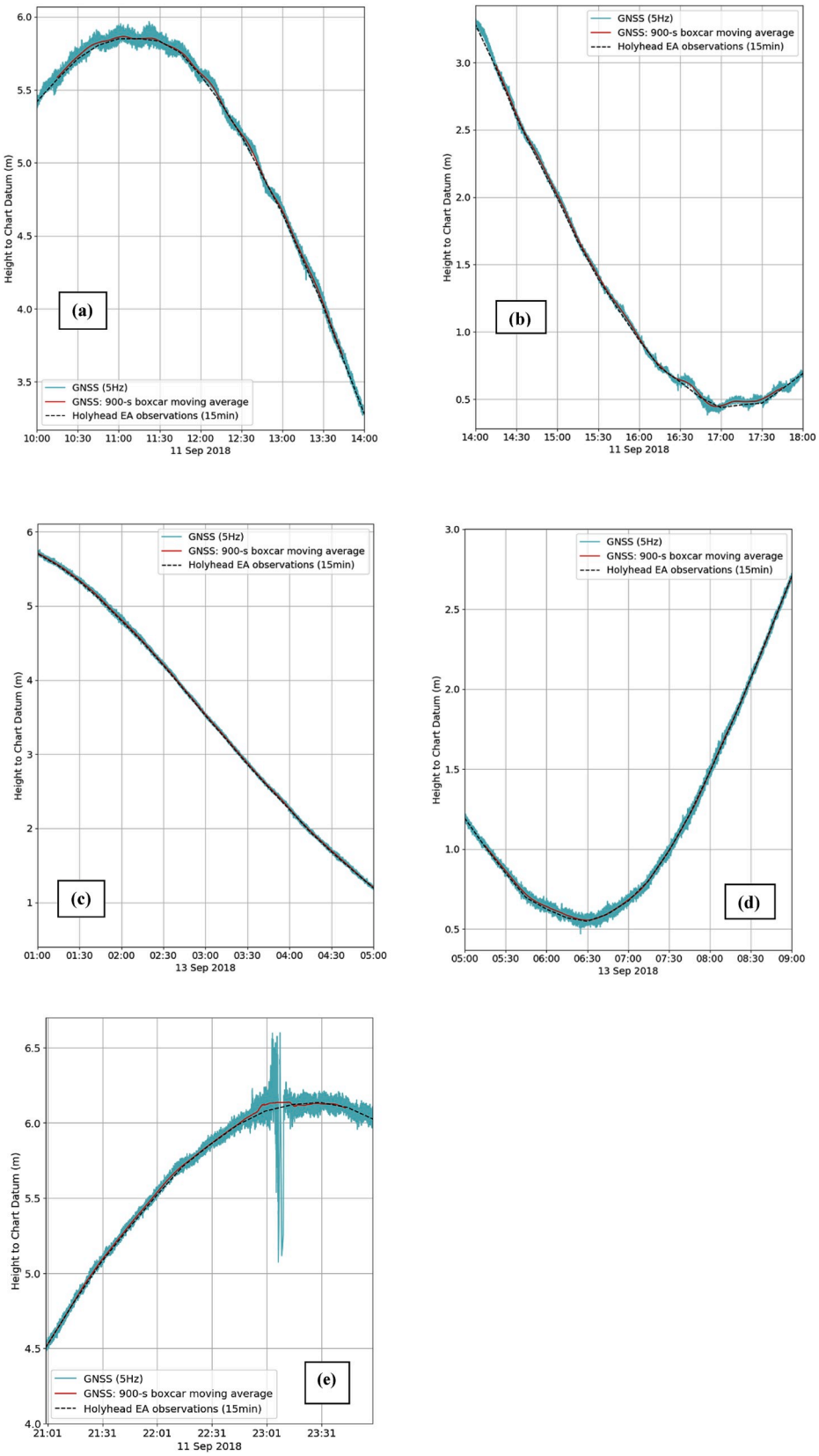

Fig. 4. Holyhead tidal elevations (a) 11 September 2018 10:00–14:00, (b) 11 September 14:00–18:00, (c) 13 September 01:00–05:00, (d) 13 September 05:00–09:00, (e) 11 September 21:00–23:59 (to illustrate discontinuity 23:02–23:10); GNSS (5 Hz), GNSS (900-s boxcar moving average) and EA tide gauge (15 min).

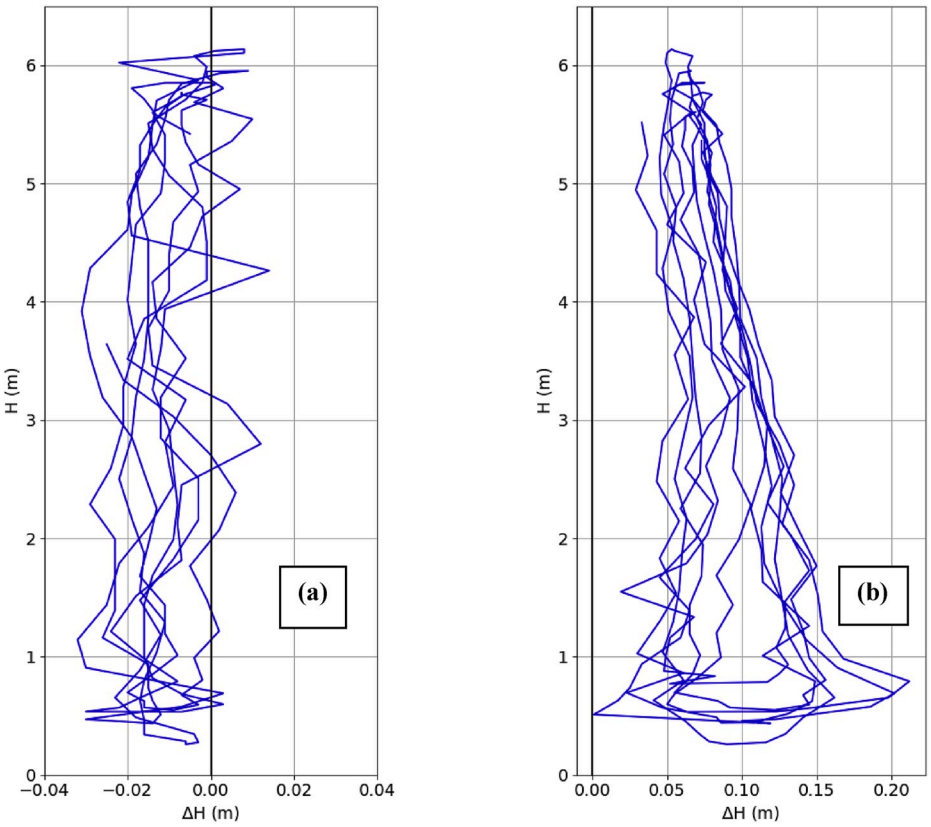

Fig. 5. Results of the Van de Casteele Test for (a) GNSS buoy 15-min averages using the EA tide gauge as a reference: differences between EA tide gauge and GNSS buoy tide gauge (ΔH) plotted against reference tide gauge (H), (b) Port Authority tide gauge 15 min averages using the EA tide gauge as a reference (for comparison). Note: Horizontal scales are different.

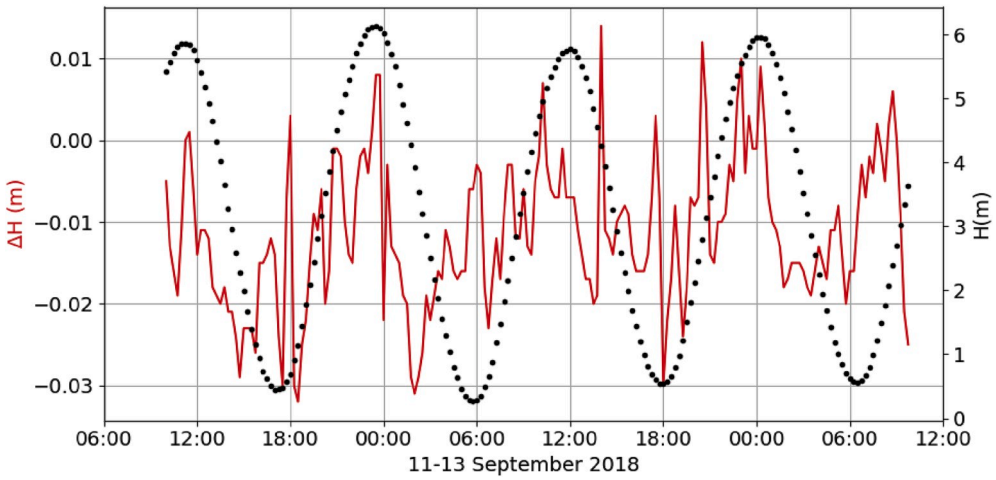

Fig. 6. Results of the Van de Casteele Test for the GNSS derived sea level data using the EA tide gauge as a reference: time series of tide gauge differences (Δ*H*, solid red line) and EA tidal observations (*H*, black dots). (For interpretation of the references to colour in this figure legend, the reader is referred to the Web version of this article.)

0.086 m, the standard deviation was 0.034 m and the RMSE was 0.092 m. However, these data confirm the presence of harbour oscillations seen within the GNSS data (Fig. 7a and b), which can be seen clearly across the high water period: 11 September 2018 at 10:00–13:00 and to a lesser degree across the high water period: 12 September 10:30–13:30. It is interesting that these oscillations are reduced in amplitude and appear to be at a different frequency during the high water period 24 h later.

The power spectral density (PSD; using Welch's method) of the 5 Hz GNSS data (in Fig. 8) indicates the presence of oscillations at frequency peaks across the 10–30 min band. Between 10:00–13:30 on 11 September, the oscillations have a period of around 22 min, while 24 h later between 10:30–13:30 on 12 September the oscillations appear to have periods of 15 and 22 min; both have similar spectral density. There appears to be more energy in the 10–30 min band spanning the high water on 11 September than on the corresponding high water on 12 September.

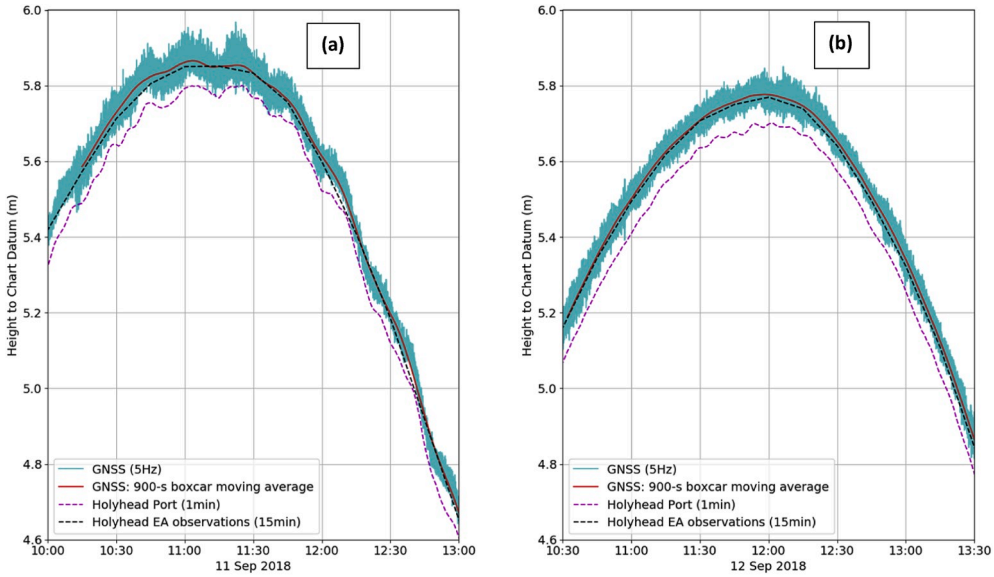

Fig. 7. Holyhead tidal elevations during (a) 11 September 2018 at 10:00–13:00, (b) 12 September 10:30–13:30. GNSS (5 Hz) in cyan, GNSS (1 min) in red, Port Authority tide gauge (1 min) in magenta and EA tide gauge (15 min) in black. (For interpretation of the references to colour in this figure legend, the reader is referred to the Web version of this article.)

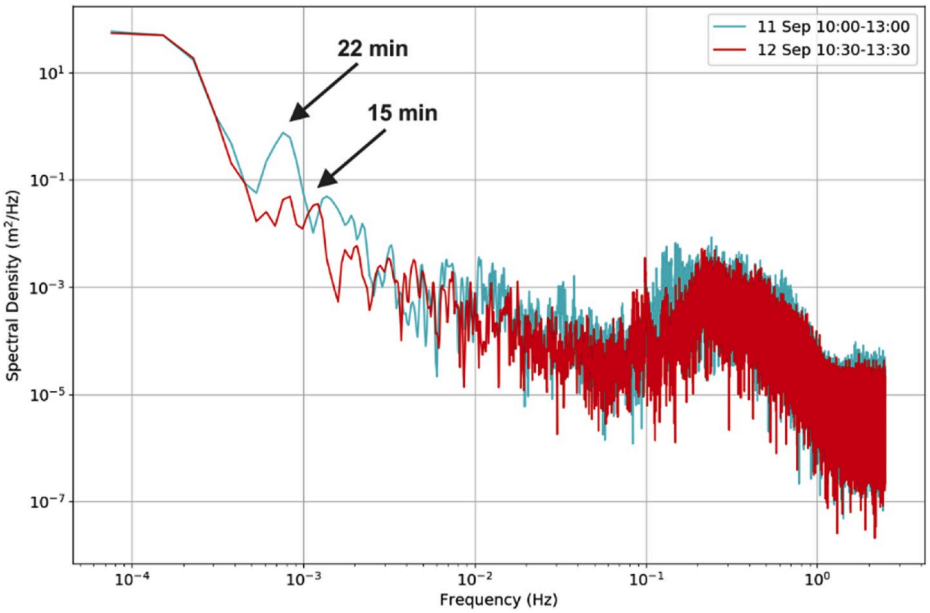

Fig. 8. Power spectral density (PSD) for the 5 Hz GNSS-derived sea level data for two 3-h periods around high water. 10:00–13:00 on 11 September 2018 in cyan, and 12 September 10:30–13:30 in red. (For interpretation of the references to colour in this figure legend, the reader is referred to the Web version of this article.)

3.4. Higher frequency oscillations

Oscillations contained within the GNSS data with periods shorter than one minute (frequencies higher than 0.0167 Hz) were explored. As well as noise introduced by the GNSS system and PPK solution method, other potential sources of the high frequency oscillations are the responses to external waves across the harbour entrance, ferry movements, and pitch and roll motion induced by response of the buoy platform to sea surface waves.

Fig. 9 shows the power spectral density of the 5 Hz GNSS-derived sea level data for the periods 11 September 10:30 to 12 September 09:35, and 12 September 10:17 to 13 September 09:51. The first period is shorter in order to avoid contaminating the spectra from the poor quality data on 11 September (23:02–23:10). There are peaks at 10 s, 8 s, and 4 s periods, which point to the presence of appreciable wave activity in the New Harbour complex. A possible cause of the waves could be the wakes of Irish Sea ferries (with an extensive daily schedule to and from Ireland) and other port traffic. On each day of the deployment, there were twenty evenly spread departures and arrivals; the longest gap with no scheduled ferry service was 3.5 h, although the ferry arrival/departure times were not always consistent with the schedule (visual note made during deployment) and other traffic were using the port. The results are consistent with other studies on ferry wakes, for example Soomere (2005) observed groups of waves created by a fast ferries operating in the Baltic Sea with periods of 9–15 s, 7–9 s and 3–4 s.

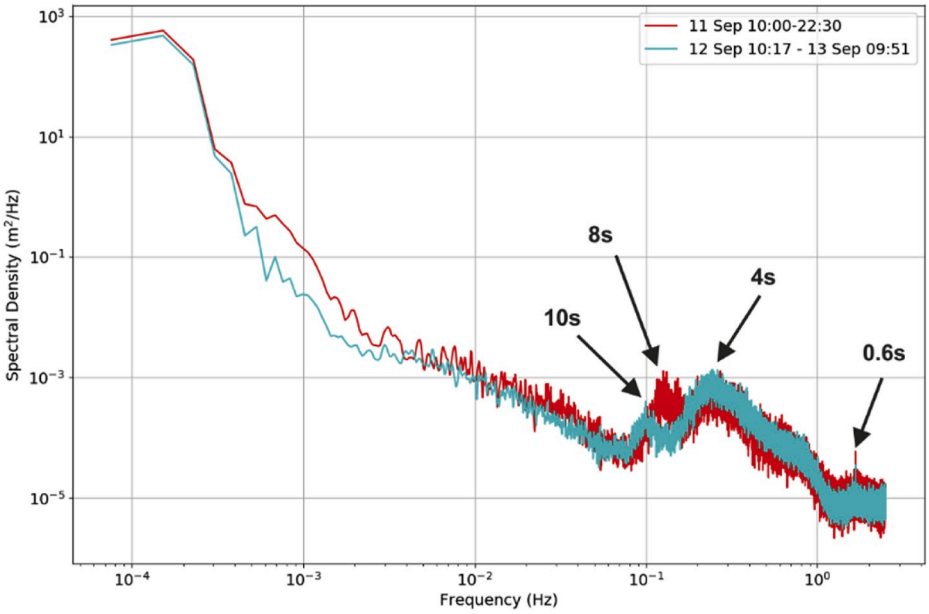

Fig. 9. Power spectral density (PSD) for the 5 Hz GNSS-derived sea level data for 11 September 10:30–12 September 09:35 in cyan, and 12 September 10:17 to 13 September 09:51 in red. Note the first period is shorter so as to avoid contaminating the spectra from the poor quality data on 11 September (23:02–23:10). (For interpretation of the references to colour in this figure legend, the reader is referred to the Web version of this article.)

3.5. Uncertainty in the derived sea level solution

The GNSS-derived sea level solution contains uncertainty related to the processing method in 'kinematic mode', which manifests itself as resembling noise (see section 2.4 on data processing). To investigate this contribution and ascertain its likely effect on the derived solution, another identical U-blox M8T receiver and antenna were positioned on the fundamental benchmark (FBM) at Holyhead for one hour, coincident with a buoy deployment. The RTKLIB software was then applied, with the parameters listed in Table 1, to obtain the vertical levels, and once again using the Ordnance Survey GNSS data as the base station. Applying the solution parameter of 'kinematic' to a receiver on a fixed point (stationary) would therefore quantify the processing noise within the kinematic solution. To compare the results, the solution parameter of 'static' was also applied to the GNSS M8T receiver data at the FBM reference station.

The power spectral densities for the three situations are shown in Fig. 10. It confirms the presence of high frequency components in the GNSS buoy results (see section 3.4). When compared with the GNSS results at the FBM, the spectra support the hypothesis of locally generated waves within the New Harbour. The two FBM power spectra highlight the differences in the solution due to the chosen processing options ('static' and 'kinematic') with the static solution having much lower energy. Differences between the mean of each FBM solution (static, kinematic) is small (less than 1 cm), and the corresponding standard deviations for each time series are 0.0024 m and 0.0097 m, respectively. Also, there is a peak of around 1 s period within the FMB (Kinematic mode) solution (Fig. 10). This may be an artefact of the RTKLIB processing software and how it copes with two different sampling rates for base and rover e.g., the GNSS buoy recorded at 5 Hz and

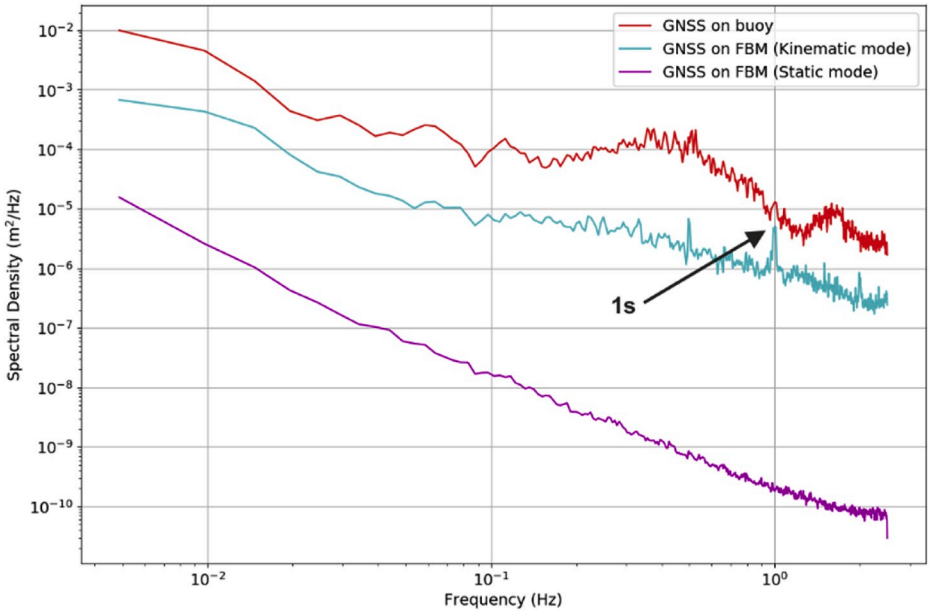

Fig. 10. Power spectral density (PSD), 5 Hz GNSS-derived vertical data for a one-hour period for a GNSS U-blox M8T located at a fixed point (the fundamental benchmark, FBM) using 'static' mode (magenta line) and 'kinematic' mode (cyan line), and on the buoy in 'kinematic' mode only (red line). (For interpretation of the references to colour in this figure legend, the reader is referred to the Web version of this article.)

the OS GNSS station data were recorded at 1 Hz.

4. Discussion and conclusions

A test deployment of an experimental buoy fitted with a GPS system (U-blox M8T GNSS receiver) for measuring coastal sea level has been undertaken in Holyhead Harbour, Wales, UK. The GNSS receiver recorded two days of 5 Hz data between 11 and 13 September 2018, encompassing four high waters and four low waters. The Van de Casteele Test results, comparing the GNSS positioning solution with the local EA tide gauge (part of the UK National Tidal Gauge Network), gave a mean difference of around 1 cm (RMSE 1.4 cm), thus confirming that this low-cost GNSS buoy tide gauge can produce coastal sea level measurements that are comparable with previous deployments of more expensive GNSS buoys for the same purpose (e.g. Rocken et al., 1990; Andre et al., 2013). The 1 cm difference may be due to many factors including the instruments themselves, tying errors and the way the subsequent data are analysed. For example, the uncertain 'antenna phase centre' on the Tallysman TW4721 antenna could produce errors up to 1 cm, as specified in the antenna documentation and, indeed, inferred from previous studies (Kelecy et al., 1994; Marcos et al., 2019). Using similar antennas for base and rover receivers would almost eliminate this problem, if the base site is first established using a geodetic GNSS receiver, and in combination with a short baseline. Also, the differences could arise from the different hydrodynamics between the New Harbour and the Inner Harbour; i.e., there is a separation of 1500 m between the GNSS buoy and the other tide gauges, with the added complexity of a jetty (which is open underneath) separating the New Harbour from the outer basin and Inner Harbour (Fig. 2). Furthermore, the uncertainty within the kinematic solution may result in a bias, although the experiment at the FBM reference station using both static and kinematic solutions suggest that this is smaller than 1 cm.

The observed harbour oscillations in the GNSS and Port Authority tidal data are likely to be seiches (Rabinovich, 2009; Pugh and Woodworth, 2014) that can be set in motion by external forces such as wave energy impinging on the harbour, wind, tide, and so on. Using Merian's formula, where the basin is open at one end, and with the length of the bay corresponding to one-quarter of a wavelength, the natural period for the basin is $\tau = 4L(gD)^{-½}$, where L is the length of the harbour, D is its average depth, and g is acceleration due to gravity. Considering the New Harbour, with L = 1800 m and D = 9 m the calculated period becomes 13 min, which is similar to the observed periods of 15 and 22 min (Fig. 8). Likewise, for the Inner Harbour (which is dredged to a 5.5 m minimum depth; with L = 800 m and D = 8 m), and the whole basin (i.e., the area of water contained within the seawall and the land towards the east (Fig. 2), with L = 3700 m and D = 10 m), the corresponding periods are 6 min and 25 min respectively. These observed oscillations (Figs. 7a and 8) may be related to tidal forcing since the deployment was at, or just after the peak spring tides.

The higher frequency oscillation peaks at ten, eight and four second periods shown in Fig. 9 are most likely caused by waves induced by the busy port traffic, e.g. ferries to and from Ireland. As mentioned previously these periods are consistent with other studies on ferry waves (Soomere, 2005). The pitch and roll of the buoy with local wind induced wavelets appear to be at much higher frequencies (visual assessment of the buoy on mooring), and this is what is possibly represented as the small peak in the PSD beyond 1 Hz e.g., approx. 0.6 s period (Fig. 9). Whilst this may be regarded as a complicating factor in the evaluation of the GNSS buoy for measuring sea level, it highlights the further potential for this instrument for capturing data on local wave climate (cf. Hein et al., 1990; Kelecy et al., 1994).

Over the last decade using GNSS receivers on buoys to measure sea levels has been prohibitively expensive when compared to other methods, and thus they have mainly been used for specific scientific purposes. However, recently the overall cost for 'geodetic quality' GNSS receivers and antennas and associated loggers has fallen dramatically and these low-cost packages can now deliver centimetre-level accuracy. For example, U-blox now offer a new dual frequency receiver (e.g., ZED-F9P) with a similar cost to the U-blox M8T used in this experiment. Furthermore, there are additional GNSS systems such as Galileo becoming fully operational, a new carrier frequency (e.g. L5), which when combined with advances in GNSS receiver software will help to reduce errors and improve the overall positional results. Consequently, the low-cost GNSS tide gauge buoy developed herein offers considerable potential for multiple deployments within survey domains and for addressing information gaps in our global network of tide gauges for monitoring coastal sea level. This potential is enhanced by the GNSS buoy tide gauge's compact size, permitting 'single person' deployment, and its low cost making it attractive for use in low and middle income countries where financial resources for environmental monitoring are limited.

Declaration of competing interest

The authors declare that they have no known competing financial interests or personal relationships that could have appeared to influence the work reported in this paper.

CRediT authorship contribution statement

Philip J. Knight: Writing - original draft, Conceptualization, Investigation, Formal analysis, Resources, Methodology, Data curation, Visualization, Software. **Cai O. Bird:** Supervision. **Alex Sinclair:** Project administration. **Andrew J. Plater:** Writing - review & editing, Supervision.

Acknowledgements

The authors would like to thank Holyhead Sailing Club for access to moorings and boat support during the experiments, Holyhead Port Authority for supplying tidal and meteorological data, the British Oceanographic Data Centre for providing UK Environment Agency tide gauge data, and Dave Jones and colleagues at the UK National Oceanography Centre for technical help and advice. Also, the services of the Natural Environment Research Council (NERC) British Isles continuous GNSS Facility (BIGF), www.bigf.ac.uk, in providing archived GNSS data (and/or products) to this study are gratefully acknowledged. The research is part of a PhD study funded by the 'Low Carbon Eco-Innovatory (LCEI) - Liverpool University' (https://www.liverpool.ac.uk/environmental-sciences/working-with-business/), with industrial partner MM Sensors Ltd. This paper is a contribution to work package 4 of the UK NERC-funded BLUEcoast project (NE/N015614/1).

References

André, G., Miguez, B.M., Ballu, V., Testut, L., Wöppelmann, G., 2013. Measuring Sea Level with GPS−equipped Buoys: a Multi−instruments Experiment at Aix Island. The International Hydrographic Review, Monte-Carlo, Monaco Principality, vol. 10. International Hydrographic Bureau, pp. 27–38.

Apel, H., Hung, N.G., Thoss, H., Schöne, T., 2012. GPS buoys for stage monitoring of large rivers. J. Hydrol 412–413, 182–192. https://doi.org/10.1016/j.jhydrol.2011.07.043.

Ballu, V., Bouin, M., Calmant, S., et al., 2009. Absolute seafloor vertical positioning using combined pressure gauge and kinematic GPS data. J. Geodyn. 84 (2010), 65. https://doi.org/10.1007/s00190-009-0345-y.

Bell, P., 2008. Mapping Shallow Water Coastal Areas Using a Standard Marine X-Band Radar, Hydro8, 4th-6th November 2008. Liverpool, International Federation of Hydrographic Societies conference paper. http://nora.nerc.ac.uk/id/eprint/5938/. (Accessed 19 July 2019).

Bell, P.S., Bird, C.O., Plater, A.J., 2016. A temporal waterline approach to mapping intertidal areas using X-band marine radar. Coast. Eng. 107, 84–101. https://doi.org/10.1016/j.coastaleng.2015.09.009.

BIGF, 2018. BIGF, NERC, British Isles continuous GNSS facility. http://www.bigf.ac.uk/. (Accessed 29 October 2018).

Bird, C.O., Bell, P.S., Plater, A.J., 2017. Application of marine radar to monitoring seasonal and event-based changes in intertidal morphology. Geomorphology 285, 1–15. https://doi.org/10.1016/j.geomorph.2017.02.002.

CDDIS, 2018. CDDIS, NASA's archive of space geodesy data. https://cddis.nasa.gov/Data_and_Derived_Products/GNSS/orbit_products.html. (Accessed 25 April 2018).
Emlid Reach, 2019. Emlid Reach M+ RTK GNSS module for precise navigation and UAV mapping. https://emlid.com/reach/. (Accessed 16 April 2019).
Frappart, F., Roussel, N., Darrozes, J., Bonneton, P., Bonneton, N., Detandt, G., Perosanz, F., Loyer, S., 2017. High rate GNSS measurements for detecting non-hydrostatic surface wave. Application to tidal bore in the Garonne River. Eur. J. Remote Sens. 49 (1), 917–932. https://doi.org/10.5721/eujrs20164948.
Harley, M.D., Turner, I.A., Short, A.D., Ranasinghe, R., 2011. Assessment and integration of conventional, RTK-GPS and image-derived beach survey methods for daily to decadal coastal monitoring. Coast. Eng. 58, 194–205.
Hein, G.W., Landau, H., Blomenhofer, H., 1990. Determination of instantaneous sea surface, wave heights, and ocean currents using satellite observations of the Global Positioning System. Mar. Geodes. 14, 217–224. https://doi.org/10.1080/15210609009379664.
Kaplan, E.D., Hegarty, C.J., 2017. Understanding GPS/GNSS, Principles and Applications, third ed. Artech House, Boston/London.
Kelecy, T.M., Born, G.H., Parke, M.E., Rocken, C., 1994. Precise mean sea level measurements using the Global Positioning System. J. Geophys. Res. 99 (C4), 7951–7959.
Lin, Y.-P., Huang, C.-J., Chen, S.-H., Doong, D.-J., Kao, C.C., 2017. Development of a GNSS buoy for monitoring water surface elevations in estuaries and coastal areas. Sensors 17 (1), 172. https://doi.org/10.3390/s17010172.
Marcos, M., Wöppelmann, G., Matthews, A., Ponte, R.M., Birol, F., Ardhuim, F., Coco, G., Santamaria-Gomez, A., Ballu, V., Testut, L., Chambers, D., Stope, J.E., 2019. coastal sea level and related fields from existing observing systems surveys in geophysics. https://doi.org/10.1007/s10712-019-09513-3.
Miguez, B.M., Testut, L., Wöppelmann, G., 2008. The van de Casteele test revisited: an efficient approach to tide gauge error characterization. J. Atmos. Ocean. Technol. 25, 1238–1244. https://doi.org/10.1175/2007JTECHO554.1.
Miguez, B., Testut, L., Wöppelmann, G., 2012. Performance of modern tide gauges: towards the mm-level accuracy. Adv. Span. Phys. Oceanogr. 221–228. https://doi.org/10.3989/scimar.03618.18A.
Morales Maqueda, M.A., Penna, N.T., Williams, S.D.P., Foden, P.R., Martin, I., Pugh, J., 2016. Water surface height determination with a GPS wave glider: a demonstration in loch ness, Scotland. J. Atmos. Ocean Techol. 33 (6), 1159–1168. https://doi.org/10.1175/JTECH-D-15-0162.1.
Nicholls, R., Wong, P.P., Burkett, J., Codignotto, J., Hay, R., McLean, S., et al., 2007. Coastal Systems and Low-Lying Areas. Climate Change 2007: Impacts, Adaptation and Vulnerability. Contribution to Working Group Ii to the 4th Assessment Report of the IPCC. Cambridge University Press, pp. 315–357.
Noll, C.E., 2010. The crustal dynamics data information system: a resource to support scientific analysis using space geodesy. Adv. Space Res. 45, 14211440. https://doi.org/10.1016/j.asr.2010.01.018.
Ordnance Survey, 2019. Rinex online data resource. https://www.ordnancesurvey.co.uk/gps/os-net-rinex-data/&ftp://rinex.ordnancesurvey.co.uk/gps/rinex. (Accessed 18 April 2019).
Penna, N.T., Morales Maqueda, M.A., Martin, I., Guo, J., Foden, P.R., 2018. sea surface height measurement using a GNSS wave glider. Geophys. Res. Lett. 45 (11), 5609–5616. https://doi.org/10.1029/2018GL077950, 2018.
POLTIPS-3, 2019. Coastal tidal software. https://noc.ac.uk/business/marine-data-products/coastal. (Accessed 29 March 2019).
Pugh, D., Woodworth, P., 2014. Sea-Level Science, Understanding Tides, Surges, Tsunamis and Mean Sea-Level Changes, second ed. Cambridge University Press, Cambridge.
Rabinovich, A., 2009. Seiches and Harbor Oscillations. In: Handbook of Coastal and Ocean Engineering, pp. 193–236. https://doi.org/10.1142/9789812819307_0009.
Rocken, C., Kelecy, T.M., Born, G.H., Young, L.E., Purcell Jr., G.H., Wolf, S.K., 1990. Measuring precise sea level from a buoy using the Global Positioning System. Geophys. Res. Lett. 17 (2), 2145–2148.
Roussel, N., Ramillien, G., Frappart, F., Darrozes, J., Gay, A., Biancale, R., Striebig, N., Hanquiez, V., Bertin, X., Allain, D., 2015. Sea level monitoring and sea state estimate using a single geodetic receiver. Rem. Sens. Environ. 171, 261–277. https://doi.org/10.1016/j.rse.2015.10.011.
RTKLIB, 2018. Open source program package for GNSS positioning 24. http://www.rtklib.com.
Soomere, T., 2005. Fast ferry traffic as a qualitatively new forcing factor of environmental processes in non-tidal sea areas: a case study in Tallinn bay, Baltic Sea. Environ. Fluid Mech. 5 (4), 293–323. https://doi.org/10.1007/s10652-005-5226-1.
Stal, C., Poppe, H., Vandenbulcke, A., De Wulf, A., 2016. Study of post-processed GNSS measurements for tidal analysis in the Belgian North Sea. Ocean Eng. 118, 165–172. https://doi.org/10.1016/j.oceaneng.2016.04.014.
Tallysman, 2019. Tallysman TW4721 performance measurements. https://www.tallysman.com/wp-content/uploads/TW4721-Measurements.pdf. (Accessed 26 June 2019).
Turvey, R., 2007. Vulnerability assessment of developing countries: the case for small-island developing states. Dev. Pol. Rev. 25 (2), 243–264.
U-blox, 2016. White paper: achieving centimeter level performance with low cost antennas. https://www.u-blox.com/en/white-papers. (Accessed 18 April 2018).
U-blox, 2019a. Product details for M8T series GNSS receivers. https://www.u-blox.com/en/product/neolea-m8t-series. (Accessed 16 April 2019).
U-blox, 2019b. Application note: GPS antennas, RF design considerations for U-blox GPS receivers. https://www.u-blox.com/sites/default/files/products/documents/GPS-Antenna_AppNote_(GPS-X-08014).pdf. (Accessed 24 May 2019).
UK Coastal Monitoring and Forecasting, 2015. Annual report for 2015 for the UK national tide gauge network. https://www.bodc.ac.uk/data/hosted_data_systems/sea_level/uk_tide_gauge_network/reports/documents/2015annualreport.pdf. (Accessed 10 June 2019).
Watson, C., Coleman, R., Handsworth, R., 2008. Coastal tide gauge calibration: a case study at Macquarie Island using GPS buoy techniques. J. Coast. Res. 24 (4), 1071–1079. https://doi.org/10.2112/07-0844.1.
Woodworth, P.L., Smith, D.E., 2003. A one year comparison of radar and bubbler tide gauges at Liverpool. Int. Hydrogr. Rev. 4, 2–9.